Model Estimates of Optical Emissions due to Lightning-induced Electron Precipitation

Robert A. Marshall, *Nicholas Lavassar*, and *Umran S. Inan*
STAR Laboratory, Stanford University, 350 Serra Mall, Stanford, CA 94305, USA; ram80unit@gmail.com

Abstract

Model calculations are conducted to estimate the optical emission brightness caused by lightning-induced electron precipitation (LEP). Pitch-angle scattering of energetic radiation-belt electrons by whistler-mode waves results in precipitation in the upper atmosphere. We calculate the secondary ionization production and optical emissions in a number of lines and bands. We find that the N_2 1P and $O(^1S)$ emissions may reach ∼10 R for a 100 kA peak current, with distinct spatial and temporal signatures. A simple SNR calculation shows that the emissions should be detectable with modern photometric instruments. We further investigate the dependence of these emissions on lightning source latitude.

1 Introduction

Intense lightning discharges emit an electromagnetic pulse (EMP) in the VLF frequency range, the intensity of which may reach 50 V/m at 100 km range (e.g., *Rakov and Uman*, 2003). Most of the EMP energy propagates in the Earth-ionosphere waveguide, but a fraction leaks through the lossy ionosphere and propagates as whistler-mode waves in the magnetosphere. In the course of their propagation, these waves will interact in cyclotron resonance with relativistic radiation belt electrons, resulting in pitch-angle scattering of these electrons. A small fraction of these electrons will be scattered into loss cone, and will be precipitated in the upper atmosphere.

Secondary ionization formed by this precipitation has been detected for decades using subionospheric VLF remote sensing, and such events are known as Trimpi or LEP events (*Helliwell*, 1965). This detection method has been used to constrain the spatial precipitation region and time signature (*Johnson et al.*, 1999). *Peter and Inan* (2007) used LEP observations to estimate the total precipitated flux of $\sim 10^{-2}$ ergs/cm^2/sec, due to a 133 kA discharge in Northwest Texas. However, the VLF subionospheric method is unable to resolve the precipitated electron energy spectra or altitude profiles. In addition to secondary ionization, LEP events will also result in optical emissions, like aurora. In this paper we estimate the brightness of those emissions to ascertain their detectability.

2 Model Description

The modeling method used in the present study is described in detail in *Marshall et al.* (2010). Our modeling effort primarily utilizes two established models. The first part follows the methodology of *Bortnik et al.* (2006a) and others. The lightning energy is broken into a spectrum, and the field intensity at the base of the ionosphere is calculated analytically, and propagated through the ionosphere to 1000 km altitude using an attenuation factor from (*Helliwell*, 1965, Fig. 3-35). From there, whistler-mode waves are ray-traced through the plasmasphere, including magnetospheric reflections and path-integrated Landau damping. Wave-particle interactions and scattering near the loss cone are calculated following the method of *Bell* (1984) but using fully relativistic equations multiple harmonic resonances. This series of calculations results in an estimate of the precipitated flux as a function of time (at 0.2 second resolution), space, and electron energy, for each frequency component in the lightning spectrum. This sequence is described in more detail by *Bortnik* (2004). The radiation belt fluxes, plasmasphere density, pitch angle distributions, and atmospheric density models used here are identical to those in Figures 1 and 2 of *Marshall et al.* (2010).

The second part of the modeling effort uses the Monte Carlo deposition model of *Lehtinen et al.* (2001). With an input precipitation flux as a function of frequency at a given time and latitude, the Monte Carlo

978-1-4244-6051-9/11/$26.00 ©2011 IEEE

model propagates electrons into the upper atmosphere and calculates the energy deposition as a function of altitude, with 1 km altitude resolution. This process is repeated for all time steps and latitudes, and the results are extended in longitude by a scaling factor (*Bortnik*, 2004, Eq. 5.5), yielding a three-dimensional volume of energy deposition, evolving in time. We then use the well-known result that each 35 eV of deposited energy produces an ionization pair *Rees* (1963). We use the excitation calculation methods of *Vallance Jones* (1974, Sec. 4.2) to find ionization and optical emission rates at each time step in the 3D volume. Finally, a geometric line-of-sight calculation through the emitting volume yields the emission brightness, in Rayleighs, observed at a predetermined location on the ground.

3 Ionization and Emission Profiles

The ray tracing and particle precipitation calculations are identical to those conducted and reported by *Bortnik* (2004); *Bortnik et al.* (2006b), except for the lightning peak current and pitch-angle distribution. Hence, the precipitated flux v. L-shell v. time results reflect those in (*Bortnik et al.*, 2006b, Figs. 2-5). The use of a square pitch-angle distribution increases the magnitude of the precipitated flux by about two orders of magnitude, and the precipitated flux increases linearly with the lightning peak current.

Following Monte Carlo calculations, Figure 1 shows the altitude profiles of secondary ionization and optical emissions (in the N_2 1P system and $O(^1D)$ 6300 Å line) as a function of time, due to precipitation at $L = 2.5$. These results are for a 100 kA discharge at a lightning source magnetic latitude of $\lambda_m = 35°$. Ionization and the N_2 1P emission rate track each other, thanks to the negligible quenching of this excited state, and the peak of ionization and emissions occurs at ∼80–90 km. The $O(^1D)$ emission, however, is orders of magnitude weaker at lower altitudes, but stronger at 250–300 km altitudes, due to its high quenching at lower altitudes (note the difference in color scale). We also observe multiple ionization peaks in time, corresponding to the multiple magnetospheric reflections. While not shown here, we also calculate optical emissions for N_2^+ 1N and $O(^1S)$ (5577 Å), which are both similar is structure to the N_2 1P, but ∼5 and ∼3 times weaker, respectively.

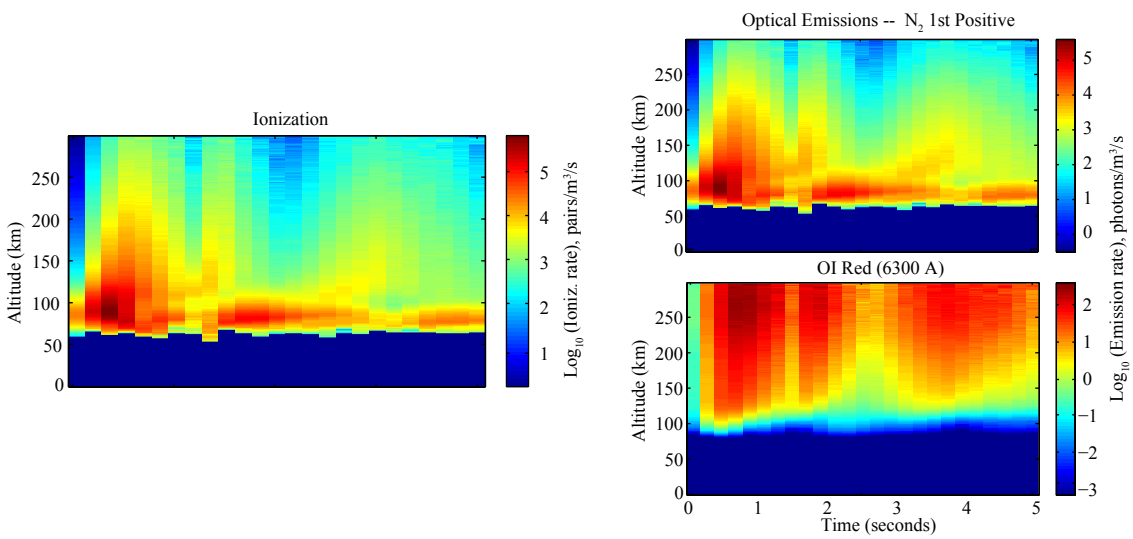

Figure 1: Ionization (top panel) and optical emission rates (bottom two panels; N_2 1P and $O(^1D)$ respectively) measured at $L = 2.5$ for a 100 kA discharge at $\lambda_m = 35°$. Note the different color scales on the bottom two panels.

Similar results are found for L-shells ranging from $L = 1.3$ to 5.5. Consistent with prior results of LEP modeling and observations, precipitation occurs first at the lowest L-shells, thanks to the shorter propagation distance, and moves towards higher L-shells with time, so that the precipitation hotspot shifts poleward over

the course of 2–3 seconds (e.g., *Johnson et al.*, 1999).

4 Camera and Photometer Signatures

We apply a geometric algorithm, integrating through the 3D emitting volume, to determine the brightness observed at some location on the ground at each time step. Figure 2 shows results for the same 100 kA discharge at 35° magnetic latitude. The top left panel in Figure 2 shows the N_2 1P brightness, integrated in altitude, at $t = 1$ s; the color scale is logarithmic, from 10^{-5} (white) to 10^{0} (red) Rayleighs. The lower left panel shows a "camera view" of these emissions at the same instant in time, for a camera placed at the location on the map. The camera view is nearly all-sky, though we have cut off the zenith portion. The top right panel shows what a photometer would measure pointed North, 15° above the horizon, as a function of time, for each of the four emissions mentioned earlier. Clearly, the N_2 1P emission is the brightest, and the $O(^1S)$ line is ∼3 times weaker. The signatures show a distinct peak near ∼1 second after the lightning discharge, consistent with the delay observed in subionospheric VLF detection of LEP. Note that the particular location chosen for the camera and photometer, and the photometer viewing direction, were taken without any optimization, and there are likely to be locations and viewing directions that are somewhat better in terms of total brightness.

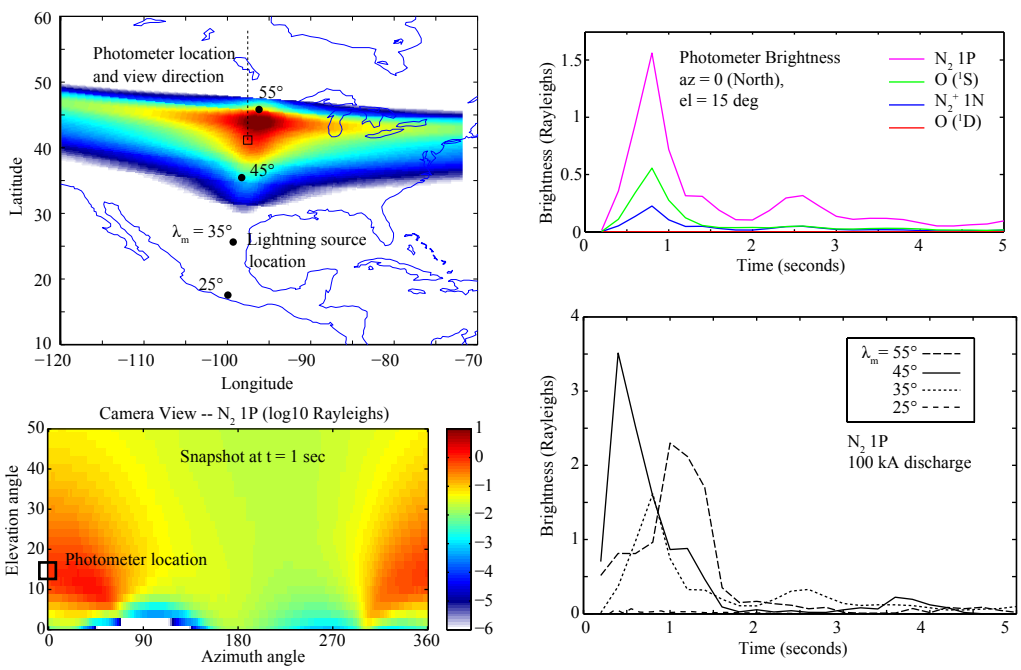

Figure 2: Results for 100 kA at $\lambda_m = 35°$. Top left: N_2 1P brightness at $t = 1$ s, integrated in altitude, with lightning and camera / photometer locations shown. Lower left: Camera view of brightness, in R, at $t = 1$ s, for N_2 1P. The $O(^1S)$ image is identical but scaled by a factor of ∼3. Top right: Photometer view, pointed North at 15° elevation, as a function of time, for N_2 1P and $O(^1S)$. Lower right: N_2 1P photometer traces with different lightning source latitudes.

The lower right panel of Figure 2 shows the photometric signatures for the N_2 1P emission for a range of source latitudes. The strongest signatures are found for lightning at higher latitudes, $\lambda_m = 45°$ and 55°. This is primarily due to the fact that at higher latitudes, the Earth's magnetic field is closer to vertical, allowing more efficient coupling of the lightning EMP into the magnetosphere. At the lowest latitudes ($\lambda_m = 25°$), the resulting emission signature has a peak of less than 0.1 R.

5 Implications for Detectability

Marshall et al. (2010) used a simple SNR calculation to determine the detectability of the optical signature of precipitation induced by VLF transmitters; here we conduct a similar calculation. For this calculation, we will investigate the O(^{1}S) green line. We assume an optical system consisting of a 75 mm aperture with a 10 × 10° field-of-view; a 12 Å filter with 50% transmission; a Hamamatsu R5900U PMT, with QE of 17%, 1 nA dark current, and 10^6 gain; and we filter the signal with 1 Hz bandwidth. We assume a typical nighttime ambient airglow at 5577 Å of 250 R *Chamberlain* (1995). Taking into account shot noise, dark noise, background noise, and amplifier noise, we find that a 1 R signal yields an SNR of ∼4.2. This SNR is dominated by the 250 R background; hence, a linear increase in signal gives a linear increase in SNR, and conditions with lower background will further improve detectability.

References

Bell, T. F. (1984), The nonlinear gyroresonance interaction between energetic electrons and coherent VLF waves propagating at an arbitrary angle with respect to the earth's magnetic-field, *J. Geophys. Res.*, *89 (A2)*, 905–918.

Bortnik, J. (2004), Precipitation of radiation belt electrons by lightning-generated magnetospherically reflecting whistler waves, Ph.D. thesis, Stanford University.

Bortnik, J., U. S. Inan, and T. F. Bell (2006a), Temporal signatures of radiation belt electron precipitation induced by lightning generated MR whistler waves. Part 1: Methodology, *J. Geophys. Res.*, *111*, A02,204, doi:10.1029/2005JA011182.

Bortnik, J., U. S. Inan, and T. F. Bell (2006b), Temporal signatures of radiation belt electron precipitation induced by lightning-generated MR whistler waves: 2. Global signatures, *J. Geophys. Res.*, *111*, A02,205.

Chamberlain, J. W. (1995), *Physics of the Aurora and Airglow*, American Geophysical Union.

Helliwell, R. A. (1965), *Whistlers and Related Ionospheric Phenomena*, Stanford University Press.

Johnson, M. P., U. S. Inan, and D. S. Lauben (1999), Subionospheric VLF signatures of oblique (nonducted) whister-induced precipitation, *Geophys. Res. Lett.*, *26*(23), 3569–3572.

Lehtinen, N. G., U. S. Inan, and T. F. Bell (2001), Effects of thunderstorm-driven runaway electrons in the conjugate hemisphere: Purple sprites, ionization enhancements, and gamma rays, *J. Geophys. Res.*, *106*(A12), 28,841–28,856.

Marshall, R. A., R. T. Newsome, N. G. Lehtinen, N. Lavassar, and U. S. Inan (2010), Optical signatures of radiation belt electron precipitation induced by ground-based VLF transmitters, *J. Geophys. Res.*, *115*, A08,206, doi:10.1029/2010JA015394.

Peter, W. B., and U. S. Inan (2007), A quantitative comparison of lightning-induced electron precipitation and VLF signal perturbations, *J. Geophys. Res.*, *112*, A12,212, doi:10.1029/2006JA012165.

Rakov, V. A., and M. A. Uman (2003), *Lightning: Physics and Effects*, Cambridge University Press.

Rees, M. H. (1963), Auroral ionization and excitation by incident energetic electrons, *Planet. Space Sci.*, *11*(10), 1209–1218.

Vallance Jones, A. (1974), *Aurora*, Reidel.